ARTICLE IN PRESS

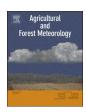
Agricultural and Forest Meteorology xxx (xxxx) xxx-xxx

FISEVIER

Contents lists available at ScienceDirect

Agricultural and Forest Meteorology

journal homepage: www.elsevier.com/locate/agrformet



Dependence of thermal roughness length on friction velocity across land cover types: A synthesis analysis using AmeriFlux data

Angela Rigden*, Dan Li, Guido Salvucci

Department of Earth and Environment, Boston University, 675 Commonwealth Ave., Boston, MA 02215, USA

ARTICLE INFO

Keywords: Thermal roughness length Excess resistance kB^{-1} Sensible heat flux

ABSTRACT

Using AmeriFlux data from 74 eddy covariance sites, we present a synthesis of the dependence of thermal roughness length on friction velocity across five land covers types, including deciduous broadleaf forests, evergreen needleleaf forests, croplands, grasslands, and shrublands. To analyze patterns in thermal roughness length, we estimate the ratio of momentum to thermal roughness lengths (kB^{-1}) at half hourly scales. Because kB^{-1} cannot be directly measured, we infer kB^{-1} from surface flux and meteorological measurements using Monin-Obukhov similarity theory. The inferred kB^{-1} is moderately correlated with the measured friction velocity over two of the land cover types—grasslands and shrublands—but weakly correlated at croplands and forests, suggesting that kB^{-1} varies with friction velocity over bluff body surfaces, but not over tightly packed, permeable canopies, such as forests and croplands. This is consistent with previous work showing contrasting turbulent structures over sparse and dense vegetation canopies. To determine how this degree of correlation affects the modeling of kB^{-1} , we estimate kB^{-1} using four common models, specifically those with friction velocity dependencies, and find that no single model works the best across land covers.

1. Introduction

Accurate estimates of turbulent fluxes of momentum, heat, and water vapor from the surface are critical for simulating atmospheric dynamics. Turbulent transport near the surface is often represented using an analogue to the transfer of electrical charge as described by Ohm's law, such that the turbulent flux and driving gradient are analogous to the electrical current and potential, respectively (Monteith and Unsworth, 2013). This resistance analogue is useful when describing turbulent fluxes as electrical current theory is well established, and facilitates the modeling of complex networks, i.e. resistance in series and/or in parallel. Using a resistance analogue, sensible heat flux (H) is described as:

$$H = \frac{-\rho c_p \cdot (T_a - T_s)}{r_{aH}} \tag{1}$$

In Eq. (1), ρ is the air density, c_p is the specific heat of air at constant pressure, T_a is the air temperature measured at height z, T_s is the temperature at the apparent source/sink height, and r_{aH} is the aerodynamic resistance to sensible heat transfer between the apparent height of the source/sink and height z.

Often, the source/sink height of heat is parameterized as a function of the sink height of momentum. For aerodynamically smooth surfaces,

the transfer of momentum and heat are both controlled by diffusive forces (i.e. viscosity). Under such conditions, the apparent source/sink heights for heat and momentum are similar. Over rough surfaces, the sink of momentum is assumed to be the height at which the extrapolated wind speed from the logarithmic profile goes to zero, or at $z_0 + d$, where z_0 is the momentum roughness height and d is the zeroplane displacement height. The source/sink height of heat is assumed to be the height at which the extrapolated temperature equals the surface radiometric temperature, or at $z_{oh} + d$, where z_{oh} is the thermal roughness height. Since pressure forces dominate the transfer of momentum while the transfer of heat remains controlled by viscous forces over rough surfaces (Thom, 1972), the sink height for momentum is typically higher than the source/sink height of heat, i.e. $z_0 > z_{oh}$, reflecting more efficient momentum transfer by pressure forces. Over vegetated or partially vegetated surfaces, the distribution of sources/ sinks of momentum and heat are also spatially variable, leading to further divergence of heat and momentum roughness lengths. In addition to structural characteristics of the vegetation (LAI, vegetation flexibility, canopy height, fraction of soil cover) modifying the distribution of sources/sinks, roughness lengths have also been found to vary with the degree of water stress and climate conditions, specifically over sparse canopies (Lhomme et al., 1997).

To account for these differences between heat and momentum

E-mail address: ajrigden@bu.edu (A. Rigden).

http://dx.doi.org/10.1016/j.agr formet. 2017.06.003

Received 1 February 2017; Received in revised form 19 May 2017; Accepted 5 June 2017 0168-1923/ © 2017 Elsevier B.V. All rights reserved.

^{*} Corresponding author.

A. Rigden et al.

transfer, heat transfer is often modeled using an excess resistance (r_b) , such that $r_{aH}(z_{oh} \to z) = r_{aH}(z_o \to z) + r_b$, where $r_a(z_o \to z)$ represents the turbulent aerodynamic resistance for heat integrated to z_o and,

$$r_b = \frac{\left[\ln\left(\frac{z_o}{z_{oh}}\right)\right]}{ku_*} \tag{2}$$

In Eq. (2), k is the von Karman constant and u^* is the friction velocity. This common representation (Eq. (2)) ignores any influence of stability corrections over the small region $z_o \rightarrow z_{oh}$. Eq. (2) is often rearranged in terms of the inverse Stanton number (B^{-1}) and the parameter kB^{-1} is defined as (Chamberlain, 1966; Owen and Thomson, 1963),

$$kB^{-1} = kr_b u_* = \ln\left(\frac{z_o}{z_{oh}}\right) \tag{3}$$

From Eq. (3), z_{oh} can be parameterized as a function of kB^{-1} , such that,

$$z_{oh} = \frac{z_o}{\exp(kB^{-1})} \tag{4}$$

As seen in Eq. (4), kB^{-1} is a parameter that acts to reduce z_0 exponentially to estimate z_{oh} . The parameter z_{oh} is a critical input to land surface models, and is especially important when estimating processes at the land surface that depend on surface temperature, such as stomatal conductance. Thus, tremendous effort has been made to parameterize this proportionality constant, kB^{-1} (see reviews by Massman, 1999; Verhoef et al., 1997); however, no universal scaling and parameterization have been agreed upon. Models of kB⁻¹ vary in complexity, including simplified parameterizations treating kB^{-1} as a constant, perhaps dependent on land cover, more complex parameterizations that depend on u_* and/or z_0 (e.g. Brutsaert, 1982; Kanda et al., 2007; Yang et al., 2008; Zilitinkevich, 1995), models that incorporate vegetation fraction, canopy structure, and/or canopy density (e.g. Blumel, 1999; Massman, 1999; Yang and Friedl, 2003), and machine learning algorithms trained on eddy covariance data (Chaney et al., 2016).

In this study, we focus on characterizing the dependence of kB^{-1} on u_{\circ} across land cover types. Our aim is not to develop a new parameterization, but to reexamine the dependence of thermal roughness length (through kB^{-1}) on friction velocity using an unprecedented amount of data. We utilize the AmeriFlux network of eddy covariance data to synthesize the relationship between kB^{-1} on u_{\circ} at evergreen needleleaf forests, broadleaf deciduous forests, croplands, grasslands, and shrublands. Our three main objectives are to (1) estimate half-hourly kB^{-1} from measured sensible heat flux and meteorological variables, (2) determine the correlation between u_{\circ} and kB^{-1} by land cover type, and (3) evaluate commonly used models of kB^{-1} . To minimize the effect of vegetation phenology on our results, we focus the analysis during the summertime, which we define as June, July, and August.

2. Materials and methods

2.1. Inferring kB^{-1} from observations

To estimate kB^{-1} , we used summertime data from 74 eddy covariance sites within the AmeriFlux data network (data available at http://www.ameriflux.lbl.gov; additionally, see link for a map of all sites). Table S1 presents the full list of sites used in this study with corresponding latitude, longitude, and land cover classification. To facilitate our analysis, we aggregated the sites by land cover types. In particular, we focused on shrublands (SHR, N (number of sites) = 8), grasslands (GRA, N = 17), croplands (CRO, N = 13), deciduous broadleaf forests (DBF, N = 11), and evergreen needle leaf forests (ENF, N = 25). In the shrubland classification, we included open shrublands, woody savannas, and savannas. Note, the "shrubland" land cover types are defined by the International Geosphere–Biosphere Programme (IGBP) as

less densely vegetated than forests, with open shrublands defined as shrub canopy cover between 10% and 60%, woody savannas as forest canopy cover between 30% and 60%, savannas as forest canopy cover between 10% and 30%. All AmeriFlux Level-2 data were processed following Rigden and Salvucci (2015).

To estimate kB^{-1} , we combined Eqs. (1) and (3), and the fact that $r_{aH}(z_{oh} \to z) = r_{aH}(z_o \to z) + r_b$, as,

$$kB^{-1} = k \cdot \left(\frac{-\rho c_p (T_a - T_{sr})}{H} - r_{aH} (z_o \to z) \right) \cdot u_*$$
(5)

In Eq. (5), T_{sr} represents the surface radiometric temperature, which was estimated primarily from upwelling longwave radiation (R_{lu}) following the Stephan Boltzmann relation as,

$$T_{sr} = \left(\frac{R_{lu} - (1 - \varepsilon)R_{ld}}{\varepsilon\sigma}\right)^{1/4} \tag{6}$$

In Eq. (6), σ is the Stefan-Boltzmann constant, ε is the emissivity, and R_{ld} is the downwelling longwave radiation. To estimate $r_{aH}(z_o \to z)$, we utilized Monin Obukhov similarity theory (Brutsaert, 2005; Garratt, 1994) neglecting the stability correction from z_{oh} to z_o , as previously mentioned, as,

$$r_{aH}(z_o \to z_m) = \frac{1}{u_* k} \left[\ln \left(\frac{z_m - d}{z_o} \right) - \Psi_h \left(\frac{z_m - d}{L} \right) + \Psi_h \left(\frac{z_o}{L} \right) \right] \tag{7}$$

In Eq. (7), z_m is the measurement height and L is the Obukhov length, defined as.

$$L = \frac{-u_*^3 \rho T_a \cdot (1 + \eta q_a) \cdot c_p}{kgH}$$
(8)

In Eq. (8), η (= 0.61) is the dimensionless ratio of the gas constants for dry air to water vapor and g is the gravitational acceleration. The Businger–Dyer stability function for heat (Ψ_h) , which accounts for deviations of the temperature profile due to stabilizing or destabilizing thermal stratification, was calculated from the dimensionless stability parameter $\xi = z_m/L$ following (Brutsaert, 2005; Garratt, 1994),

$$\Psi_h = \begin{cases} 2\ln[(1+\sqrt{1-16\xi})/2] & \xi < 0\\ -5\xi & 0 \le \xi \le 1\\ -5-5\ln(\xi) & \xi > 1 \end{cases}$$
(9)

Note, in Eqs. (5)–(9), all variables are either measured $(H, T_a, R_{lw}, \rho, q_a, u^*)$ or constants (k, g, c_p, η) except z_o, d , and ε . To estimate z_o and d, we assumed z_o to be 10% of the vegetation height (z_{veg}) and d to be 70% of z_{veg} . To more accurately characterize z_{veg} , for each site we determined the climatological monthly z_{veg} (ranging from 0 to z_m) that best predicted the measured wind speed assuming atmospheric neutrality following Pennypacker and Baldocchi (2016). To account for the effect of ε , we performed the analysis over a range of ε values from 0.94 to 0.98.

When analyzing the diurnal cycles of kB^{-1} , we excluded half-hours with counter-gradient heat fluxes, e.g. H>0 when $T_s< T_a$, which sometimes occurred during early morning and afternoon transitional periods. Friction velocities less than 0.01 m/s were also excluded from the analysis. Additionally, to minimize errors associated with small temperature gradients, we excluded half-hours when H was less than $20~\mathrm{Wm}^{-2}$. The total amount of data used in this analysis is located in Table 1. When determining the relationship between kB^{-1} and u_s , we further subsampled the data to minimize errors associated with small temperature gradients. Specifically, we subsampled the data to include only the 8 half-hours with the largest sensible heat flux for each day. Lastly, as another quantitative tool to assess the strength of the relationship between kB^{-1} , r_b , and u_s , we fit a power model to the subsampled half-hourly data, in the form $r_b = a(u_s^{P1})$ and $kB^{-1} = b(u_s^{P2})$, using a robust linear regression in the logarithmic space.

Download English Version:

https://daneshyari.com/en/article/6536869

Download Persian Version:

https://daneshyari.com/article/6536869

<u>Daneshyari.com</u>